CD47 Mediates Post-adhesive Events Required for Neutrophil Migration Across Polarized Intestinal Epithelia

Charles A. Parkos,* Sean P. Colgan,‡ Tony W. Liang, Asma Nusrat, Abraham E. Bacarra, Denice K. Carnes, and James L. Madara

Division of Gastrointestinal Pathology, Departments of *Pathology and ‡Anesthesia, Brigham and Women's Hospital, Harvard Medical School and the Harvard Digestive Diseases Center, Boston, Massachusetts 02115

Abstract. Transepithelial migration of neutrophils (PMN) is a defining characteristic of active inflammatory states of mucosal surfaces. The process of PMN transepithelial migration, while dependent on the neutrophil β_2 integrin CD11b/CD18, remains poorly understood. In these studies, we define a monoclonal antibody, C5/D5, raised against epithelial membrane preparations, which markedly inhibits PMN migration across polarized monolayers of the human intestinal epithelial cell line T84 in a bidirectional fashion. In T84 cells, the antigen defined by C5/D5 is upregulated by epithelial exposure to IFN-γ, and represents a membrane glycoprotein of ~60 kD that is expressed on the basolateral membrane. While transepithelial migration of PMN was markedly inhibited by either C5/D5 IgG or C5/D5 Fab fragments, the antibody failed to inhibit both adhesion of PMN to T84 monolayers and adhesion of isolated T84 cells to the purified PMN integrin, CD11b/CD18. Thus, epithelial-PMN interactions blocked by C5/D5 appear to be downstream from initial CD11b/CD18-mediated adhesion of PMN to epithelial cells. Purification, microsequence analysis, and cross-blotting experiments indicate that the C5/D5 antigen represents CD47, a previously cloned integral membrane glycoprotein with homology to the immunoglobulin superfamily. Expression of the CD47 epitope was confirmed on PMN and was also localized to the basolateral membrane of normal human colonic epithelial cells. While C5/D5 IgG inhibited PMN migration even in the absence of epithelia, preincubation of T84 monolayers with C5/D5 IgG followed by antibody washout also resulted in inhibition of transmigration. These results suggest the presence of both neutrophil and epithelial components to CD47-mediated transepithelial migration. Thus, CD47 represents a potential new therapeutic target for downregulating active inflammatory disease of mucosal surfaces.

ACTIVE inflammation of surfaces lined by columnar epithelia is histologically defined by transmigration of neutrophils (PMN)[1] across such epithelial monolayers and subsequent collection of PMN in the lumen (26, 53). Recently, neutrophils have been recognized not only to influence epithelial function during transmigration, but also to interact with biochemically distinct apical domains after translocation to the lumenal compartment, thus further modifying key epithelial processes (33, 51). For example, in intestinal epithelia it appears that PMN transepithelial migration may reversibly influence epithelial barrier function (19, 37, 44), while arrival in the lumenal space may result in interactions promoting electrogenic Cl^- secretion (32, 33), the known basis for secretory diarrhea (18). Thus, specific events related to the transmigration process may culminate the barrier and transport alterations characteristic of the epithelial dysfunction present in acutely inflamed mucosal surfaces.

The process by which PMN migrate across polarized columnar epithelial surfaces is only partially understood. It is increasingly clear that the paradigm that applies to PMN–endothelial interactions does not apply to PMN–epithelial interactions (42). For example, PMN interactions with epithelia and endothelia display contrasting dependencies on PMN β_2 integrins (30, 41, 43, 48) and carbohydrates (12). Such interactions are also differentially regulated by inflammatory cytokines (10, 11). Likewise, ligands crucial to transendothelial movement of PMN such as the immunoglobulin superfamily members ICAM-1 and ICAM-2, are either not expressed in columnar epithelia (ICAM-2 [14]) or are not involved in transepithelial migration of PMN (ICAM-1[10, 41]; Parkos, C. A., S. Colgan, M. Diamond, A. Nusrat, T. Liang, T. Springer, and J. Madara, manuscript in preparation). Such contrasting paradigms for PMN association with and transmigration across endothe-

Address correspondence to Charles A. Parkos, M.D., Ph.D., Department of Pathology, Brigham and Women's Hospital, 75 Francis St., Boston, MA 02115. Tel.: (617) 732-6533. FAX: (617) 732-6796.

1. *Abbreviations used in this paper*: DFP, diisopropylfluorophosphate; HUVEC, human umbilical vein endothelial cells; IAP, integrin-associated protein; NGS, normal goat serum; PMN, polymorphonuclear leukocytes.

lia versus columnar epithelia are perhaps to be expected given the markedly different microenvironments and geometries of these highly divergent systems. For example, flow-related shear, an essential consideration for extravasation of PMN that is overcome, in part, by selectin-mediated PMN endothelial interactions (5, 49, 50), has no counterpart in epithelia. Moreover, the paracellular space through which PMN must negotiate to move across these biological barriers is less than 1 μm in length for endothelia but ~25–30 μm (i.e., ~3 PMN diameters) for columnar epithelia. Hence the lateral membrane interactions between PMN and epithelia that occur during transepithelial migration may be complex. Additionally, whereas initial contact between extravasating PMN and endothelial cells is made at the apical membrane domain, first contact occurs at the basolateral domain of epithelial cells.

Another unique feature of epithelial–PMN interactions is exemplified during bacterial disease. Under such circumstances, the apical or lumenal epithelial membrane is the site of first contact with offending organisms. Recent observations indicate that, in response to such "external" challenges, columnar epithelial cells can acutely regulate and, indeed, seemingly orchestrate PMN migration responses (35, 36). Thus, it is likely that, as a consequence of the biological distinctions between PMN migration across endothelial versus epithelial surfaces, PMN–epithelial interactions might present a unique (and highly available) array of sites for application of targeted therapeutic intervention.

While the anatomy of columnar epithelia dictates complex interactions between transmigrating PMN and epithelial lateral membranes, the ligands responsible for such interactions are only beginning to be understood. The PMN integrin CD11b/CD18 is required for transepithelial migration (41). Although the counter-receptor(s) on the epithelial surface for this integrin remain undefined, they appear to be enriched on the basolateral domain (43). Candidate counter-receptor molecules do not appear to include ICAM-1 (41; Parkos, C. A., S. Colgan, M. Diamond, A. Nusrat, T. Liang, T. Springer, and J. Madara, manuscript in preparation), but are regulated in expression by cytokines such as IFN-γ (10). Given the likely complexity of lateral membrane–PMN interactions during transit across the lengthy epithelial surface, it would not be surprising if additional, CD11b/CD18-independent events also occurred during transepithelial migration.

Due to the limited current understanding of events required for PMN migration across columnar epithelial surfaces, we have raised monoclonal antibodies against membranes derived from a model polarized human intestinal epithelium and have examined the effects of such antibodies on epithelial-PMN interactions. Here we characterize one such antibody, C5/D5. In this report, we demonstrate that C5/D5 IgG inhibits the process of PMN transepithelial migration. In contrast, C5/D5 does not inhibit either initial adhesion of PMN to epithelial cells or adhesion of epithelial cells to purified CD11b/CD18. The antigen recognized by C5/D5 is a membrane glycoprotein of ~60 kD having a core peptide of ~35 kD and is basolaterally expressed on polarized human intestinal epithelial cell lines. In natural human intestine it is likewise expressed basolaterally by epithelial cells and also by lamina propria inflammatory cells. Microsequencing and cross-blotting/ELISA assays reveal the C5/D5 antigen represents a previously cloned immunoglobulin family member with an unusual predicted topology and an uncertain function (CD47). Since we show that CD47 is expressed on colonic epithelium and confirm CD47 is also expressed on PMN, experiments to probe the relative contribution(s) of each cell type in CD47-mediated transmigration were performed. While PMN-associated CD47 appears to be crucial in the process of neutrophil migration, epithelial preexposure with C5/D5 IgG also resulted in inhibition of transmigration. Such findings indicate that CD47 may be used by both epithelia and PMN during movement of PMN from the epithelial basolateral surface to the intestinal lumen.

Materials and Methods

Cell Culture

T84 cells (15, 16) were grown in a 1:1 mixture of Dulbecco's modified Eagle medium and Ham's F-12 medium supplemented with 15 mM Hepes buffer (pH 7.5), 14 mM $NaHCO_3$, 40 μg/ml penicillin, 8 μg/ml ampicillin, 90 μg/ml streptomycin, and 5% newborn calf serum. Subculturing (or preparation of suspensions and / or lysates) was performed every 6–8 d by treatment with 0.1% trypsin and 1.0 mM EDTA in Ca^{2+}- and Mg^{2+}-free phosphate-buffered saline (15). For apical-to-basolateral transmigration experiments, T84 monolayers were grown on permeable collagen-coated, polycarbonate supports (inserts) with a surface area of 0.33 cm^2 (Costar Inc., Cambridge, MA) as previously described (41). For physiologically directed, basolateral-to-apical transmigration, T84 cells were plated on the underside of permeable filters to produce inverted monolayers (31, 41). Such inverted monolayers effectively reverse the polarity of neutrophil–epithelial interactions studied by allowing gravitational settling of PMN onto the basolateral aspect of the monolayer(41).

For purification of the protein recognized by mAb C5/D5 the clonal derivative, Cl.19A, of the human intestinal epithelial cell line HT29 (2) (kindly provided by Dr. C. Laboisse, Université de Nantes, France) was grown to confluency in 165-cm^2 tissue culture flasks. Subculturing (or harvesting) was performed every 5 d by trypsin treatment with 0.1% trypsin in Ca^{2+}- and Mg^{2+}-free phosphate buffered saline. Typically, cells were split 1:10 in DME supplemented with 10% FBS, 1 mM L-glutamine, 100 U/ml penicillin, 0.1 mg/ml streptomycin (all from GIBCO BRL, Gaithersburg, MD) and became confluent within 5–6 d.

Primary cultures of human umbilical vein endothelial cells (HUVEC) were established from normal term umbilical cords as described previously (21). For experimental use, second passage cells were plated on gelatin-coated 0.33-cm^2 polycarbonate filters (Costar Corp., Cambridge, MA) and maintained in Medium 199 (with 25 mM Hepes; GIBCO BRL) supplemented with 10% FBS, 2 mM L-glutamine, 100 U/ml penicillin, 100 U/ml streptomycin, 25 μg/ml endothelial cell growth supplement (Collaborative Research Inc., Bedford, MA), 50 μg/ml heparin (Sigma, St. Louis, MO), and 250 ng/ml amphotericin B (Fungizone; GIBCO BRL) for 7 d before use.

For surface-labeling experiments by ELISA, T84 or HT29 (Cl 19.A) cells were plated 48 h before use at 3/4 confluent density in 96-well microtiter plates in cell culture media with or without 1,000 U/ml IFN-γ (kindly provided by Genentech Inc., South San Francisco, CA).

PMN Isolation

PMN were isolated from whole blood (anticoagulated with citrate/dextrose) obtained from normal human volunteers, using a gelatin sedimentation technique previously described in detail (24). PMN were resuspended in modified HBSS devoid of Ca^{2+} and Mg^{2+} (HBSS(−)) at a concentration of 4×10^7 cells/ml (4°C) and used for subsequent experiments.

Buffers

HBSS consisted of (in g/L); 0.185 $CaCl_2$, 0.098 $MgSO_4$, 0.4 KCl, 0.06 KH_2PO_4, 8 NaCl, 0.048 Na_2HPO_4, 1 glucose, and Hepes added to 10 mM (pH 7.4). HBSS(−) was prepared as HBSS but without $CaCl_2$ or $MgSO_4$.

Blocking buffer consisted of a phosphate-buffered saline containing 2 mM $MgCl_2$, 1 mM $CaCl_2$, 10 mM dextrose and 0.5% heat-treated BSA (heated to 60°C). IPPT wash buffer consisted of 400 mM NaCl, 100 mM NaF, 1 mM EDTA, 1% Triton X-100, and 10 mM Na_2HPO_4, pH 7.4. Lysis buffer was prepared as a solution of 100 mM KCl, 30 mM Na_2Cl, 2 mM EDTA, 10 mM Hepes, pH 7.4, and 2% Triton X-100. Sample buffer consisted of 2.5% SDS, 0.375 M Tris, pH 6.8, 20% glycerol, and 0.1% bromophenol blue.

Miscellaneous Biochemical Assays

Protein was assayed using the Bradford method (6), and by the BCA method as described by Pierce Chem. Co. (Rockford, IL) using bovine γ globulin as a standard. Superoxide production was measured as the superoxide dismutase inhibitable reduction of cytochrome C as previously described (40). Lactoferrin release was quantitated by ELISA as previously described (40).

Membrane Preparation

T84 epithelial membranes for immunization were prepared as described previously (25). Briefly, T84 cells, plated as monolayers on 45-cm^2 permeable supports (rings) (Costar Inc.) or on 150-cm^2 tissue culture flasks, were cooled to 4°C, washed with HBSS, and cells were scraped from the support with a teflon spatula in a small volume of homogenization buffer consisting of 0.34 M sucrose, 10 mM Hepes, pH 7.3, 1 mM ATP, 1 mM Dithiothreitol, and 0.1 mM EDTA. Scraped cells were then treated with 2.5 mM diisopropylfluorophosphate (DFP) (15 min, 4°C) followed by nitrogen cavitation (200 psi, 8 min, 4°C). The cavitate was centrifuged at 1,000 *g* to remove nuclear debris and the NaCl content of the supernatant adjusted to 1.0 M to remove peripheral membrane proteins. The resulting membrane suspension was pelleted by ultracentrifugation at 100,000 *g* for 45 min and was resuspended in homogenization buffer at an equivalent cell density of 1–2 × 10^8 per ml and stored at −80°C until further use.

Antibodies

To identify ligands important in neutrophil–epithelial interactions, monoclonal antibodies were prepared against T84 cell membranes and screened for inhibition of neutrophil–T84 interactions. Female BALBc mice were immunized by intraperitoneal injection of T84 epithelial membranes (200 μl per mouse; representing 1 × 10^7 cell equivalents emulsified with an equal volume of complete Freund's adjuvant). Two subsequent intraperitoneal immunizations were performed over the next 6 wk with the same material emulsified with incomplete adjuvant. Mice with high anti-epithelial antibody titers were given a final intravenous immunization by tail vein (50 μl T84 membranes in HBSS) and the spleen harvested for fusion 4 d later. Splenocytes were fused with P3U1 myeloma cells using 1,500 MW polyethylene glycol (Boehringer Mannheim, Germany) and resuspended in standard selection media (RPMI supplemented with 1 mM L-glutamine, 1/100 dilution of nonessential amino acids, 100 U/ml penicillin, 0.1 mg/ml streptomycin (all from GIBCO BRL), 1 mM sodium pyruvate, 10% heat inactivated FBS, and HAT (1/1,000 dilution of a stock of hypoxanthine, aminopterin and thymidine; American Type Culture Collection [ATCC], Rockville, MD). The resultant hybridomas were plated at limiting dilution and cultured in 96-well tissue culture plates in the presence of thymocytes prepared from DBA2 mice at a density of 1.2 × 10^5 splenocytes and 5 × 10^5 thymocytes per well. After ~7–10 d of growth, the supernatants from wells containing ~1-mm-sized colonies were harvested and assayed for surface reactivity with both PMN and T84 monolayers by ELISA as described below. Wells demonstrating predominantly epithelial reactivity were transferred to 24-well tissue culture plates for expansion and production of cell culture supernatant. The tissue culture supernatants were then removed and frozen in aliquots for subsequent screening in transmigration and adhesion assays described below. Hybridomas from the 24-well culture plates were frozen and stored until screening by functional assay was complete. After identification of functionally inhibitory hybridoma supernatants, the corresponding hybridomas were thawed, subcloned by limiting dilution ×3 and weaned from selection media. Antibodies were isotyped using a Dipstick Isotype Kit according to the manufacturer's instructions (GIBCO BRL) and hybridoma cells were injected into the peritoneal cavities of pristane-primed mice (2–5 × 10^6 cells per mouse) for the production of ascites fluids.

Antibodies were purified from ascitic fluid by standard procedures using proteinA–Sepharose (Sigma, St. Louis, MO) followed by dialysis against 150 mM NaCl containing 10 mM Hepes, pH 7.4. 1.5–3-mg/ml aliquots of concentrated, purified antibody were frozen for use in functional assays. $F(ab')_2$ and Fab' preparations were obtained by pepsin digestion (100 U/mg, 6 h, 37°C) followed by cysteine reduction (10 mM, 2 h, 37°C) and alkylation as described in detail elsewhere (39). Purity of antibody digests was confirmed by SDS-PAGE under reducing and nonreducing conditions.

Other commercially available antibodies were used as controls. As a positive control for inhibition of neutrophil transmigration, antibody 44a (anti-CD11b; ATCC) was used as described previously (41). Another anti-CD11b mAb that is noninhibitory but used for immunofluorescence was OKM1 (52; ATCC). Antibody W6/32 (antibody to major histocompatibility antigen class 1) served as a binding, noninhibitory control (4). Anti-CD47 (mAb BRIC 126 [3, 34]) was obtained from Biosource Intl. (Camarillo, CA).

Antibody Labeling/Immunoprecipitation

ELISA for Detecting Cell Surface Binding Antibodies. Confluent T84 monolayers in 96-well plates (~2 × 10^5 cells per well) were treated with 2 mM EDTA (4 min, 37°C) to expose basolateral epitopes (43), cooled to 4°C and incubated for 2 h with 25 μl of hybridoma supernatant or antibody solution. For neutrophil surface binding, 2 × 10^5 PMN in HBSS were placed in each well and allowed to attach and spread for 30 min (37°C) followed by cooling to 4°C and blocking nonspecific binding with cell culture media containing 10% FBS. Antibody solutions were then added as outlined above. After subsequent gentle washing with HBSS, cells were incubated with 25 μl of enzyme-conjugated secondary antibody diluted 1:1,000 in HBSS/10% goat serum (1 h, 4°C). Secondary enzyme conjugates included peroxidase for T84 cells and alkaline phosphatase for PMN. Color was developed using standard substrate assays and was read in a microtiter plate reader. In some experiments, FITC-conjugated goat anti–mouse secondary antibody was used. ELISA assays performed with such fluorescent secondary antibody were quantitated using a fluorescence microtiter plate reader (Millipore Inc., Milford, MA).

Immunofluorescence. For immunofluorescence, T84 monolayers were fixed in 3.7% paraformaldehyde in HBSS (10 min, 20°C), washed and incubated in HBSS containing 5% normal goat serum (NGS) for 30 min followed by primary antibody for 2 h (10 μg/ml in 5% NGS). After washing, monolayers were incubated with FITC-conjugated 2° antibody (1 h, 20°C; Cappel Inc., Durham, NC) and mounted in PBS-glycerol-*p*-phenylenediamine. Labeled monolayers were then viewed with a Zeiss/BioRad MRC-600 confocal fluorescence microscope. As a control for background labeling, control monolayers were incubated with comparable concentrations of normal mouse IgG and secondary antibody. Labeling was also performed on 3 μm, frozen tissue sections of human colonic mucosa obtained from fresh surgical specimens. Tissue sections, mounted on glass coverslips, were air-dried followed by fixation in 3.7% paraformaldehyde, and fluorescently labeled as above.

Flow Cytometry. PMN were analyzed for surface expression of C5/D5 antigen by flow cytometry as previously described (12) using a FACScan flow cytometer (Becton-Dickinson Immunocytometry Systems, Mountain View, CA).

Immunoprecipitation Experiments. To identify protein antigens of functionally inhibitory antibodies, immunoprecipitation experiments were performed, after cell surface labeling with biotin, on T84 and HT29 monolayers cultured on either 5-cm^2 permeable supports or on plastic. Briefly, monolayers were washed with HBSS and labeled with a solution of 1 mM sulfo-NHS biotin (Pierce Chem. Co.) in HBSS for 20 min (4°C) followed by quenching the reaction with 150 mM NH_4Cl. Each 5-cm^2 monolayer was solubilized in 1 ml of lysis buffer containing 100 mM KCl, 30 mM NaCl, 2 mM EDTA, 10 mM Hepes, pH 7.4, 2% Triton X-100 and protease inhibitors including 1.25 mM PMSF, 5 μg/ml chymostatin, 1 μg/ml each of leupeptin, pepstatin and bestatin (4°C). For cells grown in flasks, lysis buffer was added at a ratio of roughly 1 ml per 75 cm^2. The T84 cell lysate was subjected to sequential low speed (3,000 *g*, 10 min) and high speed (180,000 g, 45 min) centrifugation followed by filtration (0.2 μ filter). The filtered lysate was precleared for 2 h with 50 μl of IgG–Sepharose (mouse IgG coupled to CNBR-activated Sepharose 6 MB at a protein/Sepharose density of 3 mg/ml according to the manufacturer's instructions; Pharmacia Inc, Uppsala, Sweden) followed by incubation for 2 h (4°C) with 30 μl C5/D5–Sepharose, prepared exactly as described for the mouse IgG–Sepharose above. Immunoprecipitates were washed first in IPPT wash buffer followed by 1% octylglucoside in 100 mM sodium phosphate, pH 7.4, and finally washed in 1% octylglucoside in 20 mM sodium phosphate,

pH 7.4. The washed immunoprecipitates were denatured by heating to 100°C in the presence of 50 μl nonreduced sample buffer followed by removal of the Sepharose pellet. The denatured, solubilized immunoprecipitate was then subjected to reduced and nonreduced SDS-PAGE on linear 4–16% gradient polyacrylamide gels followed by Western blotting using standard protocols. Before SDS-PAGE, reduced samples (Dithiothreitol added to 20 mM; 100°C, 3 min) were alkylated by addition of iodoacetamide to 50 mM (100°C, 3 min) and nonreduced samples were alkylated by addition of iodoacetamide to 5 mM. Biotin surface-labeled proteins were visualized after incubation with peroxidase-conjugated streptavidin using enhanced chemiluminescence, according to the manufacturer's instructions (Amersham Inc., Buckinghamshire, UK).

For deglycosylation experiments, immunoprecipitates were denatured in buffer containing 0.5% SDS followed by addition of a sevenfold excess of NP-40. Samples were then subjected to N-linked or O-linked deglycosylation using commercially available enzymes (peptide: *N*-glycosidase F, neuraminidase and *O*-glycopeptide endo-D-galactosyl-*N*-acetyl-α-galactosamino hydrolase, respectively) exactly as described by the manufacturer (*N*-glycanase, neuraminidase, *O*-glycanase; Genzyme, Cambridge, MA).

Protein Purification and Microsequencing

Functionally active CD11b/CD18 was purified by immunoaffinity chromatography using peripheral blood leukocyte lysates exactly as previously described (17).

Immunopurification of the Antigen Defined by C5/D5 IgG. Approximately 8,500 cm^2 of Cl 19.A HT29 cells were stimulated with 1,000 U/ml IFN-γ for 48 h to increase the expression of the C5/D5 antigen. Immediately before harvesting, five 165-cm^2 flasks (~10% of the total) were transiently exposed to 2 mM EDTA in HBSS(−) to open tight junctions thereby exposing ectodomains of basolateral membrane proteins (41). The EDTA-treated cells were then surface labeled with biotin as described above. Both labeled and unlabeled flasks were then washed 3× with HBSS (4°C), and cells were isolated and pooled by scraping with a teflon spatula into ~120 ml of lysis buffer (2–3 ml of lysis buffer per flask of cells) containing 1.25 mM PMSF, 5 μg/ml chymostatin, 1 μg/ml each of leupeptin, pepstatin and bestatin (4°C) and 2 mM EDTA. Diisopropylfluorophosphate (Sigma) was then added to the lysate to achieve a final concentration of 2.5 mM and stirred for 15 min on ice. The extract was sequentially subjected to low speed (2,000 *g*, 10 min) then high speed (180,000 *g*, 45 min, 4°C) centrifugation followed by passage through a 0.2 μ filter. The extract was then pumped at a flow rate of 25 ml/h first through a column of bovine γ globulin–Sepharose (5 ml, 3 mg γ globulin per ml of beads; coupled as described in the above immunoprecipitation section; BGG–Sepharose; Sigma) followed in tandem by a column of C5/D5–Sepharose (3 ml, 3 mg IgG per ml of beads; coupled as described above). The C5/D5 column was then washed at a flow rate of 25 ml/h with IPPT wash buffer (50 ml) followed by 1% octyl glucoside in 100 mM sodium phosphate, pH 7.4 (30 ml), and finally in 1% octylglucoside in 20 mM sodium phosphate, pH 7.4 (30 ml). Bound proteins were eluted at a flow rate of 25 ml/h with a 30-ml pH gradient decreasing from pH 5.0 (150 mM NaCl and 50 mM NaOAC, 1% *n*-octylglucoside) to pH 3.0 (150 mM NaCl and 100 mM glycine/HCl, 1% *n*-octylglucoside) followed by an additional 10 ml of pH 3.0 elution buffer. Fractions of 2 ml were collected and neutralized by the addition of 0.1 ml of 2.0 M Tris, pH 8.0, and were analyzed by SDS-PAGE and Western blotting as described above.

For protein microsequence, the peak fraction of immunopurified protein was concentrated ~200-fold (Centricon 30 microconcentrator; Amicon Inc., Beverly, MA) and subsequently denatured, reduced and alkylated by the sequential addition of sample buffer containing 20 mM dithiothreitol followed by iodoacetamide to 50 mM. The sample was subjected to SDS-PAGE as a single lane on a 4–16% gradient polyacrylamide gel followed by electrophoretic transfer to polyvinylidene difluoride membrane (Immobilon-P; Millipore Inc.). The transferred protein was visualized by stain with amido black followed by excision of the band (~50 mm^2) and submission to the Harvard Microchemistry Service (Cambridge, MA) for tryptic digest and internal microsequencing as previously described (1, 27).

Transmigration Experiments

PMN transmigration experiments were performed using both standard (apical-to-basolateral migration) and inverted (basolateral-to-apical migration) T84 monolayers cultured on 0.33-cm^2 permeable supports as previously described (41). Briefly, confluent T84 monolayers were washed free of media followed by apical or basolateral addition of 50 μl of antibody solution in HBSS and incubation for 20 min (20°C). For some apical-to-basolateral transmigration experiments T84 monolayers were preexposed to 2 mM EDTA in HBSS(−) for 12 min before washing with HBSS. Such transient calcium chelation has been shown to expose basolateral ligands to the apical compartment of the transwell device without grossly altering the morphology of the epithelium (43). After a 20-min preincubation, HBSS was added (100 μl) followed by 1×10^6 PMN in 25 μl HBSS(−). Transmigration was initiated by transfer of antibody/PMN containing monolayers to 24-well tissue culture plates containing 1 ml of 1 μM fMLP in HBSS. After incubation for 110 min at 37°C, neutrophil migration across monolayers into the chemoattractant-containing lower chambers was quantitated by myeloperoxidase assay (41). In experiments examining the effect of cytokine preactivation on PMN transmigration, the cell culture media on confluent T84 monolayers was replaced with media containing maximally stimulating concentrations of IFN-γ (1,000 U/ml) or IL-4 (10 U/ml) followed by culture for 48 h as previously described (10, 11). Cytokine-activated monolayers were then washed in HBSS and used in transmigration assays.

PMN transendothelial migration using monolayers of HUVEC was assessed in a fashion exactly as described above for T84 monolayers except for the use of a 10 nM transendothelial gradient of fMLP.

In subsets of experiments, monolayers or PMN were pretreated with antibody followed by antibody washout and use in subsequent transmigration assays. In such experiments, monolayers (20°C) or PMN (2×10^6 cells/ml in HBSS(−), 4°C) were preincubated with antibody in HBSS for 30 min followed by extensive washing and subsequent transfer to transmigration assays as described above. For monolayer preincubation experiments, unbound antibody was washed out by five successive rinses in HBSS with a five minute incubation in 1 ml of HBSS after each rinse. In such experiments, each rinse was effective in reducing the unbound antibody concentration by greater than one order of magnitude thereby reducing the final concentration of unbound antibody to negligible values. Other transmigration experiments were performed on collagen coated permeable supports without any epithelial cells. In such assays, collagen coated inserts were incubated overnight in sterile tissue culture media followed by washing and placement into 24-well tissue culture plates containing 1 ml of antibody in HBSS. After addition of 0.15 ml of antibody solution and 1×10^6 PMN to the upper chamber, fMLP was added to the lower chamber to a final concentration of 10 nM. PMN transmigration was then assessed exactly as above.

Adhesion Experiments

The effects of C5/D5 IgG on neutrophil adhesion to T84 monolayers was studied using previously described methods (41). Briefly, confluent T84 monolayers on permeable supports were transiently preexposed to 2 mM EDTA in HBSS(−) for 12 min followed by washing in HBSS. To the apical surface of each monolayer, 50 μl of antibody solution in HBSS containing 100 nM fMLP was added followed by transfer of the monolayers to 24-well tissue culture plates containing 1 ml of HBSS per chamber. 2×10^6 PMN were added in 50 μl followed by centrifugation at 250 *g* for 4 min (20°C). Transwells were then allowed to incubate at 37°C for 10 min followed by washing and quantitation of adherent PMN by myeloperoxidase assay.

The effects of C5/D5 IgG on T84 cell binding to CD11b/CD18 were assayed using slightly modified, previously described methods (17). Microtiter plates were coated with functionally active CD11b/CD18 that was purified as described above. For optimal coating with CD11b/CD18, a solution of purified integrin at ≥0.1 mg/ml was diluted 15-fold with 150 mM NaCl, 2 mM $MgCl_2$, 25 mM Tris, pH 7.3, and allowed to bind to microtiter wells for 2 h (20°C). As described previously (17), nonspecific binding was blocked by incubation with a solution of blocking buffer containing 0.5% heat-treated bovine serum albumin. For cell-binding assays, trypsin/EDTA elicited T84 cells were fluorescently labeled for 10 min at 37°C by incubation with 5 μg/ml BCECF-AM (2′,7′-bis(2-carboxyethyl)-5-(and-6)-carboxyfluorescein acetoxymethyl ester; Molecular Probes, Inc., Eugene, OR).

Adhesion assays were then performed by the addition of 50 μl of antibody solution in blocking buffer to the CD11b/CD18-coated microtiter plates followed by a 20-min incubation (20°C). Labeled epithelial cells (50 μl, ~2.5×10^5 cells per well) were added followed by gentle, constant swirling for 15 min to allow antibody binding but prevent adhesion (20°C). The assay was then moved to a flat, stationary surface at 37°C for 1 h to al-

low for adhesion. To quantitate adhesion, each well was gently washed twice and total fluorescence of each well was assayed at an excitation/emission wavelength of 485/535 nm using a fluorescence microtiter plate reader (Millipore Inc.). In such assays, the percentage of applied cells adherent to purified CD11b/CD18 typically ranged from 25 to 55%. Percent adherence was calculated as the fluorescence ratio (post-wash fluorescence/prewash fluorescence) × 100.

Statistical Analysis

Data are presented as the mean ± SD and compared by Student's *t*-test or by one-way analysis of variance (ANOVA).

Results

Three fusions of splenocytes from mice immunized with T84 membranes yielded ~4,300 antibody producing clones that were screened for reactivity with both neutrophils and T84 epithelial cells. Using the differential screening approach outlined above, ~350 clones were identified that reacted primarily with the external surface of epithelial cells. Of several antibodies that were subcloned, one antibody, C5/D5 (IgG1), which was among those that inhibited neutrophil-epithelial interactions, was further characterized.

C5/D5 IgG Inhibits PMN Transepithelial Migration But Not Adhesion To Purified CD11b/CD18

The effects of C5/D5 IgG on neutrophil migration across T84 monolayers in the apical-to-basolateral or basolateral-to-apical direction are depicted in Fig. 1. As shown in *A*, PMN transepithelial migration in the apical-to-basolateral direction is markedly inhibited by C5/D5 IgG at concentrations as low as 3 μg/ml ($4.5 \pm 3.9 \times 10^4$ vs 20.5 ± 0.45 for C5/D5 vs binding control [W6/32]; $P < 0.005$). The effects of C5/D5 IgG on PMN migration in basolateral-to-apical directed transmigration (physiologically directed transmigration) are shown in *B* (Fig. 1). Again, PMN transmigration was markedly inhibited by C5/D5 IgG in the range of 3 to 12 μg/ml (11 ± 4.1 vs $36.5 \pm 8.5 \times 10^4$ for 12.5 μg/ml C5/D5 vs ctl [W6/32]; $P < 0.02$).

Since the C5/D5 epitope appeared crucial to PMN transepithelial migration and we have previously shown that transepithelial migration is modulated by cytokines such as IL-4 and IFN-γ (10, 11), we next determined whether the C5/D5 epitope was also functionally involved in transmigration after epithelial exposure to cytokines. As shown in panel C (Fig. 1), PMN transmigration across IL-4 prestimulated (10 U/ml, 48 h) T84 monolayers was also strongly inhibited by C5/D5 IgG at concentrations as low as 2 μg/ml. As shown in *D* and *E* (Fig. 1), pretreatment of T84 monolayers with IFN-γ (1,000 U/ml, 48 h), which has been shown to influence rates of PMN transmigration and regulate surface expression of as yet undefined PMN ligands (10), retained sensitivity to inhibition of PMN transmigration by C5/D5 IgG (*D*) and resulted in enhanced surface expression of the C5/D5 epitope (*E*; 250 ± 35 vs 760 ± 90 fluorescence units before and after IFN-γ stimulation, respectively; $P < 0.02$). The data in Fig. 1 *D* show mAb C5/D5 inhibits PMN migration across IFN-γ pretreated T84 monolayers irrespective of the polarity of transmigration (13.7 ± 6.3 vs $35.6 \pm 4.7 \times 10^4$ basolaterally-to-apically migrated PMN for C5/D5 IgG vs control, respectively; $P < 0.02$). Of interest, such inhibition was observed despite IFN-γ–induced downregulation of physiologically directed transmigration (10) from $63.5 \pm 4 \times 10^4$ migrated PMN in controls to $35.6 \pm 4.7 \times 10^4$ migrated PMN after IFN-γ pretreatment. As revealed in cross-comparisons of the C5/D5 IgG concentration dependence between *A*, *C*, and *D* (Fig. 1), inhibition of apical-to-basolateral directed transmigration by this antibody was comparable between control and cytokine stimulated monolayers.

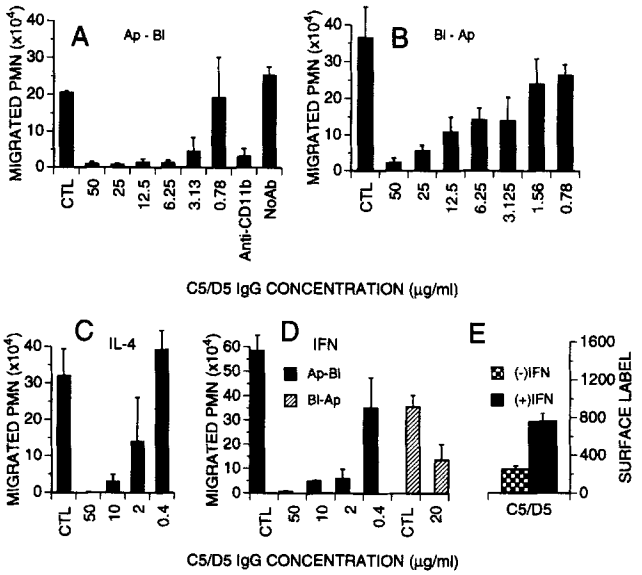

Figure 1. Functional effects of C5/D5 IgG on PMN transepithelial migration. As described in Materials and Methods, *A* and *B* represent the inhibitory effects of graded concentrations of C5/D5 IgG for PMN transmigration in the apical-to-basolateral (*Ap - Bl*) and basolateral-to-apical (*Bl - Ap*) directions, respectively. As a binding negative control antibody (*CTL*), mAb W6/32 was used at 50 μg/ml. Migration in the absence of antibody addition (*NoAb*) is shown in *A*, as is a positive control (transmigration in the presence of 5 μg/ml of inhibitory anti-CD11b/CD18 mAb 44a; reference 43). While not shown in *B*, mAb 44a inhibited transmigration by 56 ± 3%. Bars represent the mean ± SD of four monolayers for each condition (56 monolayers total). One of three experiments. (*C* and *D*) T84 monolayers were exposed to 1,000 U/ml IFN-γ or 10 U/ml IL-4, respectively, for 48 h. After cytokine washout, PMN transmigration assays were performed. For IL-4 experiments, transmigration was in the Ap-Bl direction. For IFN-γ experiments, the effects of C5/D5 IgG on transmigration are shown in both directions. In agreement with previous observations (10), IFN-γ pretreatment resulted in diminished physiologically directed transmigration from 63.5 ± 4.4 to $35.6 \pm 4.7 \times 10^4$ migrated PMN for untreated vs IFN-γ-treated T84 monolayers, respectively. Bars represent the mean ± SD of 3 monolayers for each condition (30 monolayers total). One of two experiments. (*E*) Surface expression of mAb C5/D5 epitope was assayed on control ((−)*IFN-γ*) and IFN-γ exposed ((+) *IFN-γ*) T84 cells by ELISA as described in Materials and Methods. On the Y axis, surface label represents arbitrary fluorescence units after incubation with FITC conjugated goat anti-mouse IgG. Bars represent the mean ± SD of three monolayers for each condition. One of three experiments.

Next, assays of PMN adhesion to epithelia were performed to assess whether C5/D5 inhibited an initial adhesive event as opposed to a distal transmigration event. For

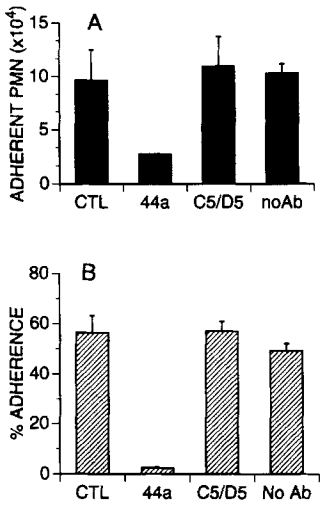

Figure 2. Effects of C5/D5 IgG on adhesion. (*A*) Neutrophil–T84 adhesion; C5/D5 IgG (25 μg/ml) was added to the apical surface of EDTA-treated T84 monolayers followed by the addition of PMN and stimulation with fMLP. Adhesion assays were then performed as previously described (41) and in Materials and Methods. As a binding, noninhibitory control, antibody W6/32 (*CTL*) was used at the same concentration. Anti-CD11b mAb 44a served as an inhibitory control as described previously (43). Adhesion in the absence of antibody is also shown (*NoAb*). (*B*) Effect of mAb C5/D5 IgG on T84 cell adhesion to purified CD11b/CD18. T84 cells, fluorescently labeled with BCECF, in the presence or absence of C5/D5 IgG (20 μg/ml) or control antibodies, were assayed for adhesion to functionally active CD11b/CD18 in 96-well microtiter plates as described in Materials and Methods. Control antibodies included W6/32 (20 μg/ml; negative inhibition), and anti-CD11b mAb 44a (10 μg/ml; positive inhibition). Bars represent the mean ± SD of four monolayers per condition in panel A and three determinations per condition in *B*. One of three experiments.

these studies (Fig. 2 *A*), a previously detailed assay that permits exposure of PMN to both apical and basolateral epithelial ligands (41) was used. Saturating concentrations of C5/D5 IgG did not inhibit adhesion of PMN to T84 monolayers thus resulting in PMN adherence values comparable to those obtained in the presence of a control binding antibody (W6/32) or in the absence of antibody (10.9 ± 2.8 vs 9.6 ± 2.8 and 10.3 ± 0.9 × 10^4 adherent PMN for C5/D5 vs W6/32 CTL and no antibody, respectively; NS). Antibody 44a, previously shown to effectively interfere with initial PMN–epithelial adhesion by blocking PMN CD11b/CD18, served as a positive control for these experiments and inhibited PMN–epithelial adhesion by greater than 70%.

Given the exquisite dependence of PMN transepithelial migration on CD11b/CD18, we next determined whether C5/D5 IgG inhibited some form of epithelial adhesive engagement of this PMN integrin. Fig. 2 *B* shows the effects of C5/D5 IgG on T84 cell adhesion to purified, functionally active CD11b/CD18. In such assays, T84 cells strongly adhere to purified CD11b/CD18 in a specific manner. As shown in Fig. 2 *B*, 56 ± 6.9% of the applied T84 cells adhered to CD11b/CD18 in the presence of a binding, control antibody, and such adherence was markedly inhibited (to 2.4 ± 0.4%) after treatment with blocking anti-CD11b antibody, 44a. In contrast to antibody 44a, preincubation of epithelial cells with saturating concentrations of C5/D5 did not influence the efficiency of epithelial cell adhesion to immobilized CD11b/CD18 (57 ± 4% of T84 cells adherent, NS). The lack of inhibition of C5/D5 IgG on T84 adhesion was not due to proteolysis of relevant epitopes by the trypsin elicitation procedure since the antibody was able to effectively surface label trypsinized T84 cells (0.579 ± 0.02 vs 0.191 ± 0.014 OD units for T84 cells labeled with C5/D5 IgG versus control mouse IgG1). As an additional test of the specificity of epithelial cell adhesion to purified CD11b/CD18, parallel assays were performed in microtiter wells coated with BSA only and showed no significant adhesion (not shown).

The inhibition of transmigration but not adhesion of PMN by mAb C5/D5 suggested the possibility of CD11b/CD18 independent, post-adhesive interactions between epithelia and PMN. If transmigration was inhibited at point(s) distal to initial adhesive events, one might expect to observe an accumulation of PMN in monolayers during transmigration assays performed in the presence of mAb C5/D5. Indeed, a frequent observation in our transmigration assays was a C5/D5 dependent increase in monolayer associated PMN (Fig. 3). While transmigration into the opposite chamber was inhibited by 68 ± 11%, there was nearly a doubling of monolayer-associated PMN after in-

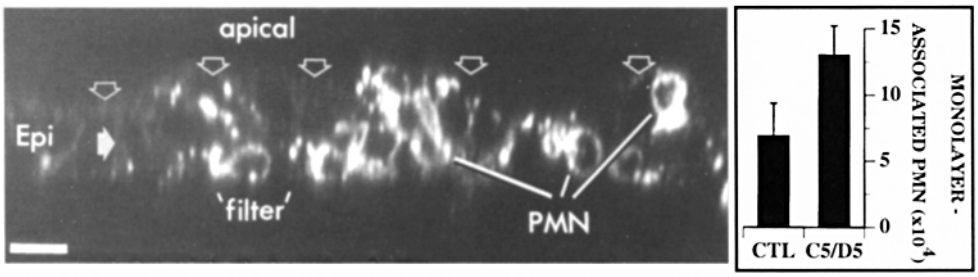

Figure 3. Effect of C5/D5 IgG on PMN migration into T84 monolayers. Basolateral to apical transmigration assays were performed in the presence or absence of 25 μg/ml C5/D5 IgG. In the graph to the right, monolayer-associated PMN were quantitated by myeloperoxidase assay as described in Materials and Methods (four monolayers each condition). Note the number of monolayer-associated PMN is nearly doubled in the presence of C5/D5. However, despite an increase in monolayer-associated PMN, migration into the opposite or lower reservoir of the transwell device was decreased by 68% (14.4 ± 5.1 vs 45.2 ± 6.8 × 10^4 migrated PMN for C5/D5 vs W6/32 CTL, respectively). To determine the position of PMN entrapped in the monolayer/filter after C5/D5 exposure, imaging studies were performed. The photomicrograph represents an x-z computer reconstructed confocal fluorescence image of a cross-section through a T84 monolayer after a PMN transmigration assay done in the presence of 25 μg/ml C5/D5 IgG and stained to visualize PMN with the CD11b mAb OKM1. The epithelium, labeled Epi, demonstrates faintly stained basolateral membranes (*solid arrow*) due to the presence of C5/D5 IgG present throughout the assay (see Fig. 9). PMN are present within the monolayer below the apical intercellular tight junction and above the filter support. Open arrows designate the apical surface of the T84 monolayer. While not shown, confocal images of monolayers after transmigration in the absence of C5/D5 showed similar patterns of PMN migration, and background staining with normal mouse IgG instead of OKM1 revealed minimal nonspecific fluorescence. Bar, 10 μm.

cubation with C5/D5 IgG (Fig. 3, *right*). The confocal fluorescence micrograph in Fig. 3 (*left*) is of a T84 monolayer after transmigration in the presence of C5/D5 IgG and demonstrates that the quantitative increase in monolayer-associated PMN correlates with the accumulation of PMN within the epithelial monolayer. These results suggest that mAb C5/D5 IgG acts by inhibiting PMN movement across the epithelium by influencing events subsequent to initial CD11b-dependent adhesive events.

The Antigen Defined by C5/D5 Is an ~60-kD Membrane Glycoprotein

Experiments were next performed to identify the antigen recognized by C5/D5 IgG. Since C5/D5 IgG recognized an extracellular ligand, polarized monolayers on permeable supports were surface labeled (apical and basolateral) with biotin, detergent solubilized and immunoprecipitated with immobilized C5/D5 IgG. The resulting immunoprecipitates were then examined by SDS-PAGE followed by Western blots probed with peroxidase conjugated avidin. As shown in Fig. 4, C5/D5 IgG specifically immunoprecipitates a membrane protein appearing as a broad band centered at ~60 kD under reducing conditions (lane *2*) and with a similar, perhaps slightly larger (~60–65 kD), apparent molecular mass under nonreducing conditions (lane *1*). Deglycosylation experiments revealed that removal of N-linked sugar residues with treatment by peptide/N glycosidase F caused a marked reduction in the apparent molecular mass to ~35 kD. When this deglycosylated immunoprecipitate was subsequently subjected to conditions that remove O-linked sugars (*O*-glycanase) no further reduction in molecular mass was apparent (lane *4*). Although reduced and alkylated, the immunopurified protein occasionally exhibited a "laddering effect," presumably due to oligomerization (Fig. 4, lane *5* where a more lightly labeled band of molecular mass ~100 kD is apparent). Thus, the antigen defined by mAb C5/D5 is a membrane protein with an apparent molecular mass of ~60 kD, is heavily glycosylated with N-linked carbohydrate and has a core polypeptide molecular mass of ~35 kD.

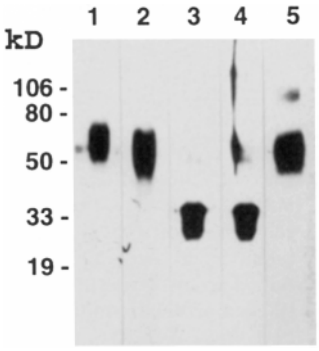

Figure 4. Immunoprecipitation of the antigen defined by C5/D5. T84 cells, grown on 5-cm^2 inserts, were biotinylated, solubilized and immunoprecipitated with immobilized C5/D5 IgG as described in Materials and Methods. Samples were then subjected to SDS-PAGE on 4–16% gradient polyacrylamide gels followed by Western blot, incubation with streptavidin-peroxidase and development by enhanced chemiluminescence. Lane *1*, nonreduced C5/D5 immunoprecipitate; lane *2*, reduced C5/D5 immunoprecipitate; lane *3*, C5/D5 immunoprecipitate subjected to N-linked deglycosylation (see Materials and Methods); lane *4*, N-linked deglycosylated C5/D5 immunoprecipitate subsequently subjected to O-linked deglycosylation (see Materials and Methods); lane *5*, C5/D5 immunoprecipitate, reduced and alkylated, but showing oligomerization.

Purification, Microsequence, and Identification of the C5/D5 Antigen as CD47

HT29 cells (subclone Cl 19.A) were used to bulk purify the antigen recognized by C5/D5. Cl 19.A cells are a well differentiated human intestinal epithelial cell line with growth characteristics more logistically suited for large-scale tissue culture compared to the relatively slow growing T84 cells. The surface expression of the C5/D5 antigen, assessed by ELISA, on Cl 19.A HT29 cells is shown in Fig. 5 and, as with T84 cells, is shown to be responsive to IFN-γ (48 h, 1,000 U/ml). An approximately twofold increase in surface expression of the C5/D5 antigen was induced by this cytokine and paralleled increased MHC class I expression. Moreover, C5/D5 immunoprecipitates obtained from Cl 19.A HT29 cells, like those obtained from T84 cells, revealed a broad ~60-kD band. While IFN-γ stimulation increased the yield of the antigen, there was no effect on the molecular mass of the immunoprecipitate (not shown).

Approximately 8,500 cm^2 of IFN-γ–activated Cl 19.A HT29 cells were used to obtain sufficient quantities of the C5/D5 antigen for microsequence. From 219 mg of crude Cl 19.A HT29 cell lysate, ~50–75 μg of purified protein was obtained, representing an overall purification of ~3,000-fold. Fig. 6 shows the avidin blot (*A*) and silver stain (*B*) of the purified material eluted from the C5/D5–Sepharose using a decreasing pH gradient. As can be seen in Fig. 6 *A*, a single biotin-labeled protein band was obtained that was indistinguishable from the immunoprecipitate shown in Fig. 4, lane *2*. Silver stain of the corresponding unconcentrated fractions confirmed purification to apparent homogeneity revealing a single protein band with a reduced apparent molecular mass of ~60 kD (*B*).

The peak protein containing fraction (Fig. 6, *fraction 13*) was concentrated, subjected to SDS-PAGE and electro-

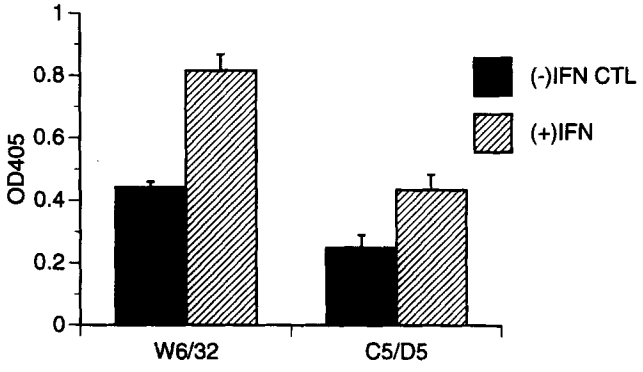

Figure 5. Expression of the C5/D5 antigen on Cl 19.A HT29 cells. Surface expression of mAb C5/D5 epitope was assayed on control ((−)*IFN-γ*) and IFN-γ stimulated ((+) *IFN-γ*) Cl 19.A HT29 cells by ELISA as described in Materials and Methods. On the Y axis, surface label is represented by optical density units after substrate addition. Specific labeling was determined by subtracting the optical density of monolayers incubated in normal mouse IgG. W6/32 IgG, which strongly labels epithelial cells, was used as a binding control antibody at 20 μg/ml. Bars represent the mean ± SD of quadruplicates. One of two experiments.

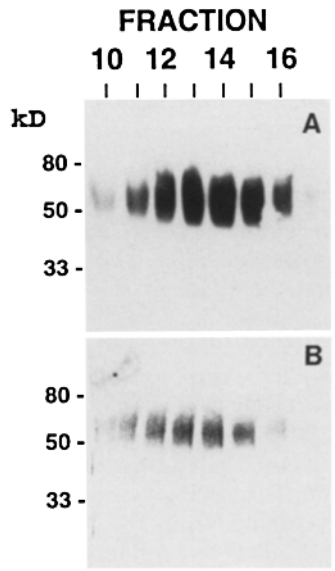

Figure 6. Purification of the antigen defined by C5/D5. Approximately 8,500 cm^2 of Cl 19.A HT29 cells were exposed to IFN-γ (1,000 U/ml, 48 h) and subsequently biotinylated, solubilized and passed through a column of immobilized C5/D5 IgG as described in Materials and Methods. Bound protein was eluted with a pH gradient decreasing from pH 5 to pH 3 and fractions of 2 ml were collected and neutralized as described in Materials and Methods. Both panels represent SDS-PAGE of reduced and alkylated column fractions (25 μl) on 4–16% polyacrylamide gradient gels. Bound protein was observed to elute at pH values below 4.0. *A* represents a Western blot of the column eluate fractions developed by enhanced chemiluminescence after incubation with streptavidin-peroxidase. *B* represents the silver-stained SDS gel of the column eluate fractions.

phoretically transferred onto a PVDF membrane followed by protein staining with amido black. Limited amino acid composition revealed ~124 pmol of protein immobilized on the PVDF membrane. Two different tryptic peptides were isolated by HPLC and sequenced yielding the following sequences: IEVSQLLK and STVPTDF(S)(S)A (where parentheses indicate residues determined with lower confidence). Searches for sequence homology using GenBank/EMBL revealed a complete match for both peptides with a membrane protein referred to as OVTL3 (8) or integrin-associated protein (IAP) (28), previously determined to be identical to CD47 (29, 34). In addition to providing 100% identity with CD47, the GenBank search yielded no other significant sequence homology. Fig. 7 shows the alignment of the two peptide sequences we obtained with that of CD47. In the lower half of Fig. 7 is a hypothetical secondary structural model first proposed by Lindberg et al. (28) with the location of the two peptide sequences shown. To confirm the homology between the antigens defined by C5/D5 and CD47, an ELISA and Western blots were performed. Using microtiter wells coated with immunopurified C5/D5 antigen, the binding of C5/D5 IgG and commercially available anti-CD47 antibody (BRIC 126) were compared (Fig. 8 *A*). As can be seen in Fig. 8 *A*, both C5/D5 IgG and anti-CD47 react strongly with the immunopurified material. Such cross-reactivity was also confirmed by Western blotting of the commercially available anti-CD47 antibody against the immunopurified C5/D5 antigen (not shown).

The identification of the C5/D5 antigen as CD47 was surprising given its broad tissue distribution and the fact that hybridomas were initially screened for preferential binding to epithelial cells over PMN. The initial screening assays for the C5/D5 hybridoma suggested a low amount of surface labeling of T84 cells (~0.1 OD unit above background) and even lower amounts on PMN. It is possible that the sensitivity of the screening ELISA may have been limited for hybridoma supernatants with low antibody concentrations. Given the published reports of CD47 on PMN (7, 28, 29, 34, 45), we tested C5/D5 for reactivity with human neutrophils. As shown in Fig. 8 *B*, flow cytometry of purified, nonpermeabilized human neutrophils using C5/D5 IgG revealed substantial surface labeling with mean channel fluorescence values of 1 and 257 for control versus C5/D5-labeled PMN, respectively. Furthermore, immunopurification of the C5/D5 antigen from 10 g of PMN revealed a broadly staining protein band of ~60 kD that was indistinguishable from that obtained from epithelial cells (not shown).

Localization of C5/D5 Antigen in Intestinal Epithelia and Mucosa

Fig. 9 shows the results of immunostaining experiments, performed with C5/D5 IgG, on polarized T84 cells and on frozen sections of human colonic mucosa. As shown in *A* and *C*, there was minimal background staining with irrelevant IgG in T84 monolayers or frozen colonic tissue sections, respectively. In contrast, as shown in *B*, the en face

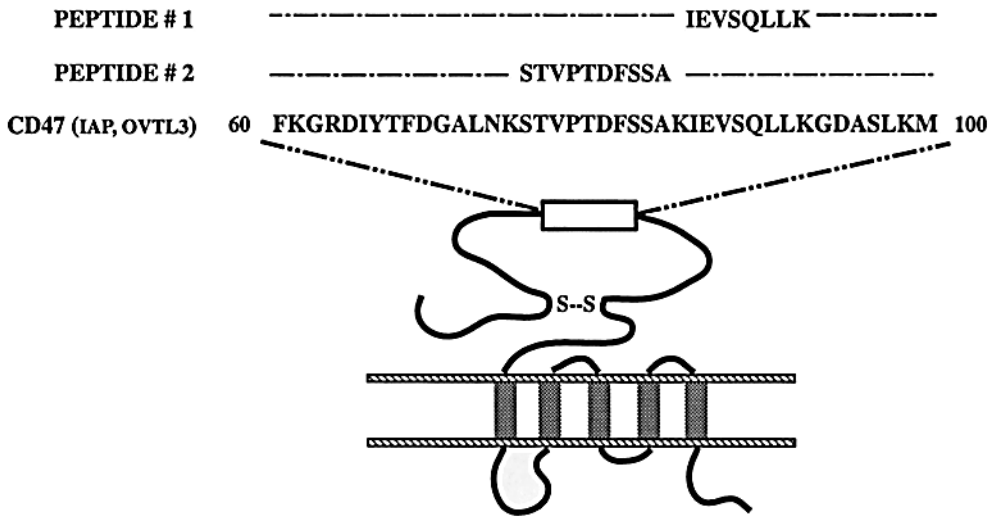

Figure 7. Alignment of peptide sequences of the C5/D5 antigen with the predicted sequence of CD47. The amino acid sequences obtained from two tryptic peptides of protein immunopurified from C5/D5 IgG are shown in alignment with the predicted extracellular immunoglobulin V-like domain of CD47 (IAP) between residues 60 and 100. The region of homology is expanded from the hypothetical secondary structure as previously reported (28).

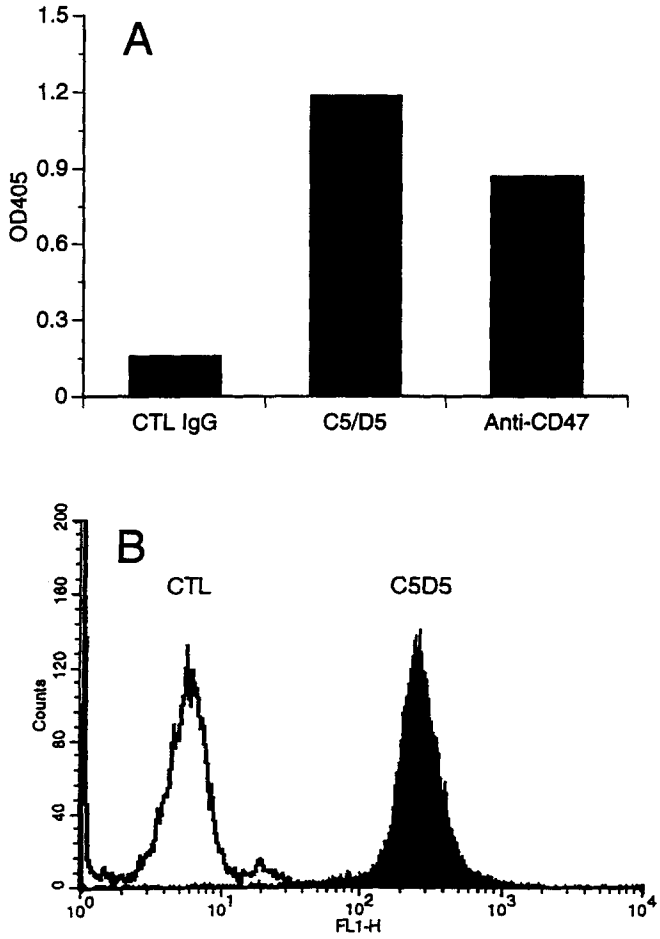

Figure 8. The antigen recognized by C5/D5 IgG is CD47 and is expressed on neutrophils. (*A*) Binding of anti-CD47 to the antigen defined by C5/D5 IgG. As described in Fig. 6 and in Materials and Methods, immobilized C5/D5 IgG was used to immunopurify the corresponding antigen. A standard ELISA was then performed on microtiter wells coated with the purified material that had been diluted 15-fold with PBS and allowed to bind nonspecifically to the surface (2 h, 20°C). Primary antibodies included C5/D5 IgG as a positive control (1 μg/ml) and a 1:10 dilution of commercially available anti-human CD47 (BRIC 126). Optical density (*OD*) is shown after substrate addition to alkaline phosphatase-conjugated secondary antibody. Nonspecific background is shown in the lane labeled CTL IgG and represents incubation with irrelevant mouse IgG. Each bar represents the average of duplicate determinations. One of two experiments. (*B*) Assessment of C5/D5 antigen on PMN by flow cytometry. PMN were stained using mAb C5/D5 or no primary Ab (*CTL*) followed by FITC-labeled goat anti-mouse antibody. Histograms represent specifically stained cell numbers on the vertical axis (labeled counts) plotted against fluorescence on a log scale from 20,000 cells per condition. One of two experiments.

fluorescent staining pattern on T84 cell monolayers viewed in a subjunctional plane reveals a typical "chicken wire" or basolateral staining pattern. While the apical surface of T84 cells showed very little staining with C5/D5 IgG, permeabilization of monolayers after fixation resulted in significant intracellular staining (not shown). To confirm the relevance of the localization findings in T84 cells, similar studies were performed on 1 μm frozen sections of normal human colon. As shown in Fig. 9 *D*, strong labeling of the basolateral aspect of normal human colonic epithelium (labeled *E*) was observed. Also in agreement with the staining results on T84 monolayers, *D* indicates a lack of staining on the apical surface of natural human colonic epithelium. In addition, panel D demonstrates labeling of mononuclear cells in the lamina propria. The majority of the lamina propria cells staining with the antibody appear to be leukocytes.

Relative Contributions of Neutrophil and Epithelial C5/D5 Antigen (CD47) to Transepithelial Migration

Since it is clear that the antigen defined by mAb C5/D5 is expressed by both epithelia and PMN, experiments were performed to determine the relative contributions of epithelial versus PMN CD47 on transepithelial migration. To exclude the possibility that C5/D5 IgG influenced transmigration by cross-linking epithelial cells to PMN, experiments using Fab′ fragments of C5/D5 IgG were performed (Fig. 10). PMN transepithelial migration in the absence of antibody was no different than migration in the presence of a control binding antibody W6/32 or the same concentration of $F(ab')_2$ and Fab′ prepared from normal mouse IgG (27 ± 4.2 vs 27.3 ± 4.1, 25.2 ± 1.2, and $23.8 \pm 4 \times 10^4$ migrated PMN for no antibody vs W6/32, CTL $F(ab')_2$ and Fab′, respectively, NS). In contrast, transmigration in the presence of C5/D5 $F(ab')_2$ and Fab′ was inhibited by 93 and 85%, respectively (25.2 ± 1.2 vs $1.7 \pm 0.7 \times 10^4$ and 23.8 ± 4 vs $3.6 \pm 0.5 \times 10^4$ migrated PMN for CTL vs C5/D5 $F(ab')_2$ and CTL vs C5/D5 Fab, respectively; $P < 0.01$). Such results effectively rule out inhibition caused by antibody mediated PMN–epithelial cross-linking or antibody mediated interactions with PMN Fc receptors.

Having excluded Fc and/or cross-linking mediated interactions as possible mechanisms of the observed inhibitory effects of C5/D5 on PMN transepithelial migration, experiments were performed to determine the relative contribution(s) of epithelial versus PMN CD47 to the transepithelial migration response. In such experiments, PMN or T84 monolayers were first preincubated with control or C5/D5 IgG and then extensively washed in HBSS to remove unbound mAb. Washed, antibody pretreated cells were then used in standard transmigration assays. As shown in Fig. 11 *A*, preincubation of inverted T84 monolayers with C5/D5 IgG resulted in 90 and 72% inhibition of transmigration when compared to antibody controls (20.4 ± 1.7 vs 2 ± 0.6 and $5.8 \pm 2.9 \times 10^4$ migrated PMN for CTL vs 50 and 25 μg/ml C5/D5 IgG preincubation, respectively; $P < 0.005$). However, as shown in Fig. 11 *B*, preincubation of PMN with C5/D5 IgG was also highly effective in inhibiting subsequent transepithelial migration (23.8 ± 2.3 vs $0.08 \pm 2.17 \times 10^4$ migrated PMN for CTL vs C5/D5 IgG preincubation, respectively; $P < 0.001$). Such results suggest that both PMN and epithelial-associated CD47 may play roles in PMN transepithelial migration. The possibility that C5/D5 could directly affect PMN migration was confirmed in assays of the effects of C5/D5 on fMLP (10 nM gradient) induced PMN migration across acellular, collagen-coated permeable supports. As shown in Fig. 11 *C*, transmigration of PMN across filters in the absence of epithelia was also effectively inhibited by C5/D5 IgG (26.9 ± 0.61 vs $1.28 \pm 0.1 \times 10^4$ migrated PMN for CTL vs

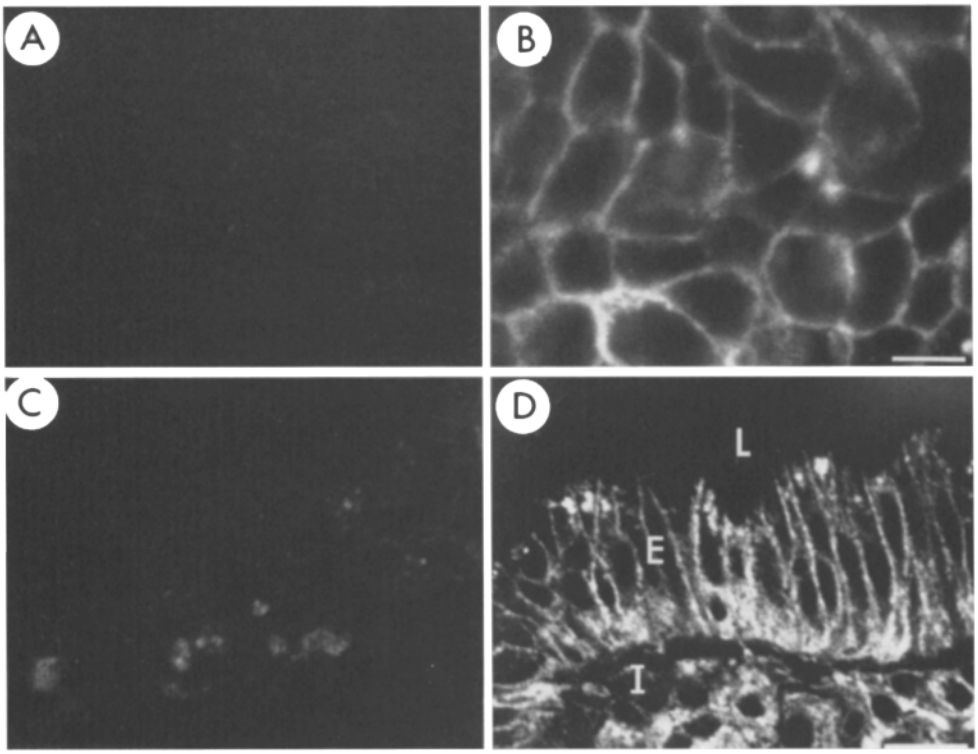

Figure 9. Immunofluorescent labeling of T84 monolayers and normal human intestine with C5/D5 IgG. (*A* and *B*) paraformaldehyde fixed T84 monolayers were incubated with C5/D5 IgG for 1 h (10 μg/ml) followed by labeling with FITC conjugated secondary antibody as described in Materials and Methods. Mounted, stained monolayers were then visualized by fluorescence confocal microscopy. *A* represents the control, stained with normal mouse IgG. *B* represents an X-Y fluorescence image in the mid-zone (subjunctional) of a T84 monolayer stained with C5/D5 that shows a chicken wire or basolateral membrane staining pattern. (*C* and *D*) Paraformaldehyde-fixed 3 μm frozen sections of human colon labeled with C5/D5 IgG followed by FITC-conjugated secondary as described above and in Materials and Methods. Panel C represents the nonspecific staining control using normal mouse IgG. *D* represents C5/D5 staining of colonic crypts and lamina propria leukocytes. *L* designates the colonic lumen that is closest to the apical aspect of the intestinal epithelium designated *E*. Note the strong labeling of the basal and lateral aspects of the epithelium and absence of labeling of the apical surface. Beneath the epithelium is the interstitium (*I*) or lamina propria that shows abundant inflammatory cells staining positively with C5/D5 IgG. Bar, 10 μm.

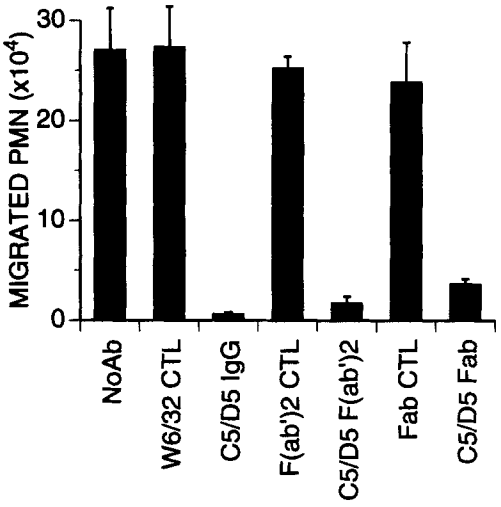

Figure 10. C5/D5 Fab'/F(ab')$_2$ fragments inhibit PMN transepithelial migration. Fab'(25 μg/ml) and F(ab')$_2$ (20 μg/ml) fragments of C5/D5 IgG were prepared by pepsin digestion and assayed for effects on apical-to-basolateral transmigration using EDTA pretreated T84 monolayers as described in Fig. 1 and in Materials and Methods. As controls, normal mouse IgG1 was pepsin digested in parallel with C5/D5 to make F(ab')$_2$/Fab. In addition, intact C5/D5 (*C5/D5 IgG*) and W6/32 were used (25 μg/ml). Bars represent the mean of 4 ± SD monolayers for each condition (28 monolayers total). One of two experiments.

migration in the presence of C5/D5 IgG, respectively; $P < 0.001$).

Experiments were also performed both to examine the selectivity of C5/D5-mediated inhibition of neutrophil function and to exclude the possibility that C5/D5-mediated inhibition of PMN migration was a consequence of C5/D5-mediated activation (i.e., due to desensitization). As shown in Table I, treatment of PMN with saturating concentrations of C5/D5 IgG did not influence PMN superoxide production or degranulation. In the presence of antibody, addition of saturating concentrations of fMLP resulted in superoxide production that was indistinguishable from that in the absence of antibody. Furthermore, addition of C5/D5 IgG failed to induce the release of primary or secondary granules, nor did it augment or inhibit degranulation after stimulation with fMLP.

Effects of C5/D5 IgG on Transendothelial Migration

Since it was recently reported that integrin associated protein (CD47) plays a role in transendothelial migration (13) we tested C5/D5 for effects on PMN migration across monolayers of HUVECS. As shown in Fig. 12, migration of PMN across monolayers of HUVECS was markedly inhibited (91%) by C5/D5 IgG (3.8 ± 2.7 vs $45.8 \pm 4.4 \times 10^4$ migrated PMN for C5/D5 vs W6/32 ctl, respectively; $P < 0.001$).

Discussion

Since little is known about the molecular interactions be-

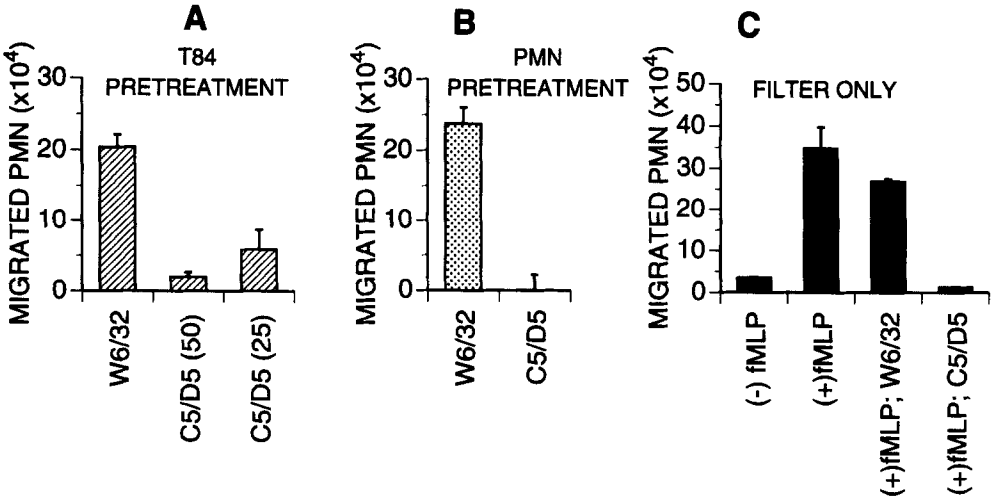

Figure 11. Relative contributions of neutrophil versus epithelial CD47 to PMN transepithelial migration. (*A*) C5/D5 IgG at the concentrations in parentheses (μg/ml) was preincubated with inverted T84 monolayers (20°C, 1 h) before extensive washing followed by immediate use in basolateral-to-apical transmigration assays as described in Materials and Methods. As a control, monolayers were preincubated with 50 μg/ml W6/32 IgG. (*B*) PMN were preincubated with equivalent doses of C5/D5 IgG or the binding, noninhibitory control antibody W6/32 (25 μg/ml) before extensive washing followed by immediate use in basolateral-to-apical transmigration assays as described in Materials and Methods. (*C*) Collagen-coated permeable supports preincubated in media overnight were used in transmigration assays as above except that antibody (10 μg/ml) was present in both the upper and lower chambers. Migration is shown in the absence ((−)*fMLP*) or presence ((+)*fMLP*) of a 10-nM fMLP transwell gradient. In the presence of an fMLP gradient, transmigration in the presence of a control binding antibody W6/32 is compared to that in the presence of C5/D5 IgG. Bars represent the mean ± SD of four monolayers for each condition (36 monolayers total). One of two experiments.

tween PMN and columnar epithelia during transepithelial migration, experiments were performed to obtain probes useful in further characterizing this important process. In this study we have raised and characterized a monoclonal antibody, C5/D5, which largely abolishes the ability of PMN to cross monolayers of the polarized crypt-like human intestinal epithelial cell line, T84. Although CD11b/CD18-mediated PMN adhesion to the epithelial surface appears to mediate initial contacts between PMN and columnar epithelial cells (41) and is required for consummation of the transmigration response (43), the C5/D5 antigen does not appear to represent a ligand for CD11b/CD18. The C5/D5 antigen is shown to represent CD47, an unusual member of the immunoglobulin superfamily. In keeping with the broad tissue distribution of CD47, previously reported to be expressed on leukocytes, platelets, endothelial cells, placenta, ovarian cancer cells, and variably on epithelia (7, 8, 20, 34), we now report CD47 expression on the basolateral surface of human colonic epithelial cells (cultured lines and natural tissue). Lastly, we provide evidence that implicates contributions of both PMN and epithelial-derived CD47 in the process of transepithelial migration.

Table I. Effect of C5/D5 IgG on Neutrophil O_2- Production and Degranulation

Condition*	Oxidase activity‡ (nmol O_2-/ 10^6 PMN)	2° Granules; lactoferrin§	1° Granules; myeloperoxidase§
C5/D5 IgG	0	0.12	0.02
C5/D5 + fMLP	8.8	0.96	0.03
fMLP	9.3	0.97	0.03
PMA	15.8	1.49	0.03
W6/32	0	0.13	0.03
W6/32 + fMLP	9.0	0.73	0.03
PMN only	0	0.12	0.03
dHCB + fMLP			0.74
Solubilized PMN			1.49

*Suspensions of 10^6/ml PMN were preincubated for 10 min with 10 μg/ml C5/D5 IgG or control W6/32 IgG before stimulation for 5 min with fMLP (100 nM). Controls included stimulation with fMLP alone (5 min), PMA alone (5 min; 100 ng/ml) or preincubation with dihydrocytochalasin B (*dHCB*) (4 min at 5 μg/ml) followed by fMLP (5 min).

‡For O_2- assays, PMN were suspended in cytocrome C buffer in presence or absence of superoxide dismutase and catalase, and stimulated for 5 min. The superoxide dismutase inhibitable reduction of cytochrome C was then determined on the cell-free supernatants as described in Materials and Methods.

§Lactoferrin was determined by ELISA, and myeloperoxidase by enzymatic activity as described in Materials and Methods. Values represent optical density after substrate addition.

Each value was determined from 1 ml of cells (10^6 PMN). One of two experiments.

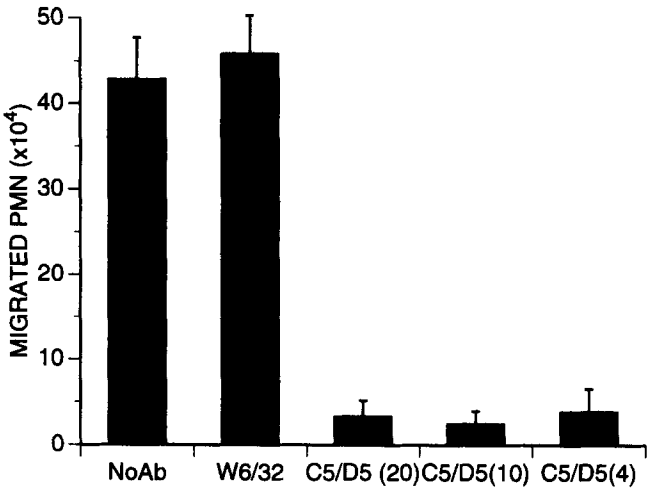

Figure 12. C5/D5 IgG inhibits PMN transendothelial migration. Dose responses of C5/D5 IgG on PMN across monolayers of HUVECs were performed exactly as described in Fig. 1 and in Materials and Methods. The concentration of antibody in μg/ml is shown in parentheses. As controls, transmigration in the absence of antibody (*NoAb*) and W6/32 (20 μg/ml) are shown. Each bar represents the mean ± SD of triplicate determinations. One of two experiments.

The molecule classified as CD47 was first cloned as an ovarian tumor marker (8) using the monoclonal antibody OVLT3 as a tool. The OVLT3 antibody was of interest since it recognized an epitope on ovarian carcinoma that was initially thought to be rarely found on normal human tissues (8). The identical sequence was subsequently obtained in studies aimed at identifying an IAP; so named since it appeared to associate with integrins from the β_3 family (7, 28). Studies initially defining IAP were as elegant as they were complex. Human PMN were observed to express a ligand binding specificity for Arg-Gly-Asp sequences that were blocked by monoclonal antibody B6H12. B6H12 immunoprecipitated an integrin-like heterodimer from surface-labeled PMN and platelets (22). The integrin-like protein appearing in B6H12 immunoprecipitates was termed the leukocyte response integrin which, while potentially displaying unusual and interesting functional characteristics, remains structurally uncharacterized (9, 23, 47, 54). However, B6H12 immunoprecipitates derived from placenta contain the $\alpha_v\beta_3$ integrin and those from platelets contain a protein that appears to be β_3 (7), raising the possibility that the integrin-like molecule in the PMN-derived immunoprecipitates is related to the β_3 integrin family. Consistent with the proposed connection between IAP and the β_3 family were a series of observations that indicate that B6H12 is able to inhibit $\alpha_v\beta_3$-mediated binding of erythroleukemia cells to vitronectin-coated beads (28). However, subsequent to the original immunoprecipitation studies (22), it became clear that the integrin-like heterodimer present in immunoprecipitates obtained using B6H12 represented coprecipitating proteins that did not directly possess the epitope recognized by B6H12. Rather B6H12 recognized a smaller protein for which the term IAP was subsequently applied (7). The antigen recognized by B6H12 (IAP) was subsequently cloned and recognized to represent CD47 (28, 29).

A structural model of CD47 has been presented by Brown and colleagues (28) and consists of: a single amino terminus, an IgV-like extracellular domain harboring several potential N-glycosylation sites, five putative membrane spanning domains, and a cytoplasmic carboxy terminus. As shown in Fig. 7, the sequences obtained in the current study are expressed in the IgV-like domain. Given the multiple membrane spanning domains, and the ability of the B6H12 antibody to interfere with vitronectin binding (an event that involves Ca^{2+} signaling), it has been speculated that B6H12 might be involved in signal transduction, perhaps even as a calcium channel (46). Currently, there is little direct evidence to support this interesting proposal. However, monoclonal antibodies to CD47 are able to inhibit fibronectin-stimulated signaling responses in human umbilical vein endothelial cells without interfering with endothelial adhesion to fibronectin-coated plastic (46). Thus, it appears that CD47 antibodies might, under specific circumstances, be able to uncouple adhesion from downstream signaling responses.

Although the precise role(s) that CD47 might play in cell regulation/signaling/etc. remain to be defined, this study and a recent report investigating neutrophil-endothelial interactions suggest that this protein may also influence such cell–cell interactions. Cooper et al. (13) have recently reported that the B6H12 antibody inhibits PMN movement across endothelial monolayers in response to gradients of fMLP and IL-8 or in response to endothelial TNFα exposure. Interestingly, while exposure of either PMN or endothelial cells to B6H12 inhibited PMN migration across TNFα stimulated HUVECS, endothelial exposure to this antibody only partially inhibited IL-8–induced transmigration. Since PMN exposure to the antibody fully inhibited transmigration in response to IL-8, these investigators concluded that both PMN- and endothelial-associated CD47 may play a role in transendothelial migration of PMN. In this report, we confirm the importance of CD47 in transendothelial migration as demonstrated by the marked inhibitory effect of C5/D5 IgG on PMN migration across monolayers of HUVECS in response to fMLP. In addition, we demonstrate that the inhibitory effects observed with C5/D5 are not mediated by Fc interactions or cell–cell cross-linking due to shared epitopes.

Given the columnar height of intestinal epithelial cells, migration of PMN across the paracellular space may be complex, and it is unclear at what "step" the C5/D5 mediated inhibition occurs. Since C5/D5 IgG failed to inhibit PMN–epithelial adhesion or T84 cell adhesion to CD11b/CD18, it appears that the CD47-mediated event(s) occur distal to at least one CD11b/CD18-dependent adhesive in-

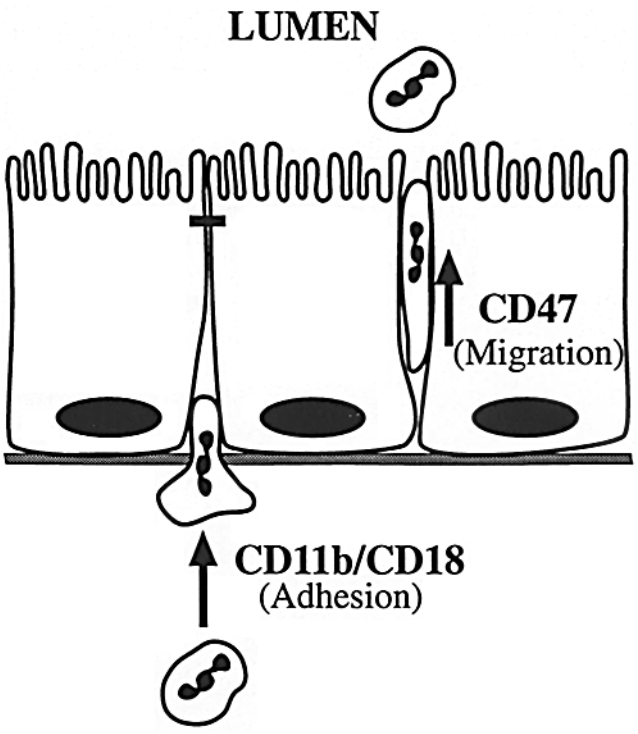

Figure 13. Multistep model of neutrophil transepithelial migration. Neutrophil migration across intestinal epithelium naturally occurs in the basolateral-to-apical direction and leads to reversible disruption of tight junctions (denoted by the heavy bar between center and left cell) and ultimately results in collection of PMN on the lumenal surface (termed crypt abscess by histopathologists). An initial adhesive event involves PMN adhesion to the epithelial cell basolateral domain and is dependent on CD11b/CD18 (41, 43) whereas a subsequent event occurring during migration of PMN between epithelial cells is dependent on CD47 (current study).

teraction. Such results might be schematized as in Fig. 13. In this multistep model of transepithelial migration, PMN, after extravasation, initially adhere to the basolateral aspect of intestinal epithelial cells in a CD11b/CD18-mediated fashion. Such events are readily captured in modified epithelial–PMN adhesion assays (41) or in assays of epithelial adhesion to purified CD11b/CD18. Subsequently, PMN migrate over the extended lateral surface of intestinal epithelial cells in a manner that is dependent, at least in part, on CD47. Transmigrating PMN then disrupt the tight junction (37, 38) and enter the lumen of the crypt, forming a crypt abscess. Such a model would predict that inhibition of CD47-mediated transmigration might cause an accumulation of PMN within the epithelium. Indeed, as shown in Fig. 3, we have observed increased monolayer-associated PMN in our transwell assays using C5/D5 IgG. Such findings, however, have always been accompanied by dramatic inhibition of the flux of PMN into the lower reservoir of the transwell device.

The precise role of epithelial-derived CD47 in PMN transepithelial migration is not clear. These results might be explained if CD47 was involved in homeotypic adhesive interactions between PMN and epithelia. However, we have failed to demonstrate adhesion of T84 cells to CD47 purified by different immunoaffinity techniques. The current observations suggest that epithelial CD47 may indeed contribute to the efficiency of PMN movement across epithelia. It is quite clear that events mediated by PMN-associated CD47 are required for successful completion of transepithelial migration. Understanding how CD47 mediates this process will require a more fundamental knowledge of the functional role this membrane protein serves in eukaryotic cells.

The authors would like to thank S. Carlson for expert assistance in the preparation of figures for this manuscript, Drs. K. Case and W. Atkinson for kindly providing human endothelial cells, Dr. C. Laboisse for providing Cl 19.A HT29 cells and Dr. W. Lane and Harvard Microchemistry for expert assistance on protein microsequencing.

This work was supported by a research grant from the Crohn's and Colitis Foundation of America, and by National Institutes of Health Grants HL54229, DK47662, DK7662, DK 35932, and DK33506.

Received for publication 19 September 1995 and in revised form 10 November 1995.

References

1. Aebersold, R., H. J. Leavitt, R. A. Saavedra, L. E. Hood, and S. B. H. Kent. 1987. Internal amino acid sequence analysis of proteins separated by one or two-dimensional gel electrophoresis after in situ protease digestion on nitrocellulose. *Proc. Natl. Acad. Sci. USA.* 84:6940–6974.
2. Augeron, C., and C. Laboisse, L. 1984. Emergence of permanently differentiated cell clones in a human colonic cancer cell line in culture after treatment with sodium butyrate. *Cancer Research.* 44:3961–3969.
3. Avent, N., P. A. Judson, S. F. Parsons, G. Mallinson, D. J. Anstee, M. J. Tanner, P. R. Evans, E. Hodges, A. G. Maciver, and C. Holmes. 1988. Monoclonal antibodies that recognize different membrane proteins that are deficient in Rh null human erythrocytes. One group of antibodies reacts with a variety of cells and tissues whereas the other group is erythroid-specific. *Biochem. J.* 251:499–505.
4. Barnstable, C. J., W. F. Bodmer, G. Brown, G. Galfre, C. Milstein, A. F. Williams, and A. Ziegler. 1978. Production of monoclonal antibodies to group A erythrocytes, HLA and other human cell surface antigens—new tools for genetic analysis. *Cell.* 14:9–20.
5. Bevilacqua, M. P., S. Stengelin, M. A. Gimbrone, and B. Seed. 1989. Endothelial leukocyte adhesion molecule-1: an inducible receptor for neutrophils related to complement regulatory proteins and lectins. *Science (Wash. DC).* 243:1160–1165.
6. Bradford, M. 1976. A rapid and sensitive method for the quantitation of microgram quantities of protein utilizing the principle of protein–dye binding. *Anal. Biochem.* 72:248–254.
7. Brown, E., L. Hooper, T. Ho, and H. Gresham. 1990. Integrin-associated protein: a 50-kD plasma membrane antigen physically and functionally associated with integrins. *J. Cell Biol.* 111:2785–2794.
8. Campbell, I. G., P. S. Freemont, W. Foulkes, and J. Trowsdale. 1992. An ovarian tumor marker with homology to vaccinia virus contains an IgV-like region and multiple transmembrane domains. *Cancer Res.* 52:5416–5420.
9. Carreno, M. P., H. D. Gresham, and E. J. Brown. 1993. Isolation of leukocyte response integrin: a novel RGD-binding protein involved in regulation of phagocytic function. *Clin. Immunol. Immunopathol.* 69:43–51.
10. Colgan, S. P., C. A. Parkos, C. Delp, M. A. Arnaout, and J. L. Madara. 1993. Neutrophil migration across cultured intestinal epithelial monolayers is modulated by epithelial exposure to IFN-γ in a highly polarized fashion. *J. Cell. Biol.* 120:785–798.
11. Colgan, S. P., M. P. Resnick, C. A. Parkos, A. E. Bacarra, C. Delp-Archer, P. W. Weller, and J. L. Madara. 1994. Interleukin-4 directly modulates function of a model intestinal epithelia. *J. Immunol.* 153:2122–2129.
12. Colgan, S. P., C. A. Parkos, D. K. McGuirk, H. R. Brady, A. A. Papayianni, G. Frendl, and J. L. Madara. 1995. Receptors involved in carbohydrate binding modulate intestinal epithelial-neutrophil interactions. *J. Biol. Chem.* 270:10531–10539.
13. Cooper, D., F. P. Lindberg, J. R. Gamble, E. J. Brown, and M. A. Vadas. 1995. Transendothelial migration of neutrophils involves integrin-associated protein (CD47). *Proc. Natl. Acad. Sci. USA.* 92:3978–3982.
14. de Fourgerolles, A., S. A. Stacker, R. Schwarting, and T. A. Springer. 1991. Characterization of ICAM-2 and evidence for a third counter-receptor for LFA-1. *J. Exp. Med.* 174:253–267.
15. Dharmsathaphorn, K., and J. L. Madara. 1990. Established cell lines as model systems for electrolyte transport studies. *Methods Enzymol.* 192: 354–389.
16. Dharmsathaphorn, K., K. G. Mandel, J. McRoberts, L. D. Tisdale, and H. Masui. 1984. A human colonic tumor cell line that maintains vectorial electrolyte transport. *Am. J. Physiol.* 246:6204–6208.
17. Diamond, M. S., D. E. Staunton, A. R. de Fougerolles, S. A. Stacker, J. Garcia-Aguilar, M. L. Hibbs, and T. A. Springer. 1990. ICAM-1 (CD54): a counter-receptor for Mac-1 (CD11b/CD18). *J. Cell Biol.* 111:3129–3139.
18. Donowitz, M., and M. J. Welsh. 1987. *In* Physiology of the Gastrointestinal Tract. Vol. 2. L. R. Johnson, editor. Raven Press, NY. 1351–1388.
19. Evans, C. W., J. E. Taylor, J. D. Walker, and N. L. Simmons. 1983. Transepithelial chemotaxis of rat peritoneal exudate cells. *Br. J. Exp. Pathol.* 64:644–654.
20. Favaloro, E. J. 1993. Differential expression of surface antigens on activated endothelium. *Immunol. Cell Biol.* 71:571–581.
21. Gimbrone, M. A. 1976. Culture of vascular endothelium. *In* Progress in Hemostasis and Thrombosis. T. Spaet, editor. Grune & Stratton Inc., NY. 1–28.
22. Gresham, H. D., J. L. Goodwin, P. M. Allen, D. C. Anderson, and E. J. Brown, 1989. A novel member of the integrin receptor family mediates Arg-Gly-Asp-stimulated neutrophil phagocytosis. *J. Cell Biol.* 108:1935–1943.
23. Gresham, H. D., S. P. Adams, and E. J. Brown. 1992. Ligand binding specificity of the leukocyte response integrin expressed by human neutrophils. *J. Biol. Chem.* 267:13895–13902.
24. Henson, P., and Z. G. Oades. 1975. Stimulation of human neutrophils by soluble and insoluble immunoglobulin aggregates. *J. Clin. Invest.* 56: 1053–1061.
25. Kaoutzani, P., C. A. Parkos, C. Delp-Archer, and J. L. Madara. 1993. Isolation of plasma membrane fractions from the intestinal epithelial model T84. *Am. J. Physiol. 264 (Cell Physiol.).* 33:C1327–C1335.
26. Kumar, N. B., T. T. Nostrant, and H. D. Appelman. 1982. The histopathologic spectrum of acute self-limited colitis (acute infectious type colitis). *Am. J. Surg. Pathol.* 6:523–529.
27. Lane, W. S., A. Galat, M. W. Harding, and S. L. Schreiber. 1991. Complete amino acid sequence of the FK106 and rapamycin binding protein, FKBP, isolated from calf thymus. *J. Prot. Chem.* 10:151–160.
28. Lindberg, F. P., H. D. Gresham, E. Schwarz, and E. J. Brown. 1993. Molecular cloning of integrin-associated protein: an immunoglobulin family member with multiple membrane-spanning domains implicated in alpha v beta 3-dependent ligand binding. *J. Cell Biol.* 123:485–496.
29. Lindberg, F. P., D. M. Lublin, M. J. Telen, R. A. Veile, Y. E. Miller, H. Donis-Keller, and E. J. Brown. 1994. Rh-related antigen CD47 is the signal-transducer integrin-associated protein. *J. Biol. Chem.* 269:1567–1570.
30. Lo, S. K., G. A. van Seventer, S. Levin, and S. D. Wright. 1989. Two leukocyte receptors (CD11a/CD18 and CD11b/CD18) mediate transient adhesion to endothelium by binding to different ligands. *J. Immunol.* 143: 3325–3329.
31. Madara, J. L., S. P. Colgan, A. Nusrat, C. Delp, and C. A. Parkos. 1992. A simple approach to measurement of electrical parameters of cultured epithelial monolayers: use in assessing neutrophil epithelial interactions. *J. Tiss. Cult. Methods.* 14:209–216.
32. Madara, J. L., C. A. Parkos, S. P. Colgan, R. J. MacLeod, S. Nash, J. Matthews, C. Delp, and W. S. Lencer. 1992. Cl^- secretion in a model intestinal epithelium induced by a neutrophil-derived secretagogue. *J. Clin. Invest.* 89:1938–1944.

33. Madara, J. L., T. W. Patapoff, B. Gillece-Castro, S. P. Colgan, C. A. Parkos, C. Delp, and R. J. Mrsny. 1993. 5'-AMP is the neutrophil-derived paracrine factor that elicits chloride secretion from T84 epithelial monolayers. *J. Clin. Invest.* 91:2320–2325.
34. Mawby, W. J., C. H. Holmes, D. J. Anstee, F. A. Spring, and M. J. Tanner. 1994. Isolation and characterization of CD47 glycoprotein: a multispanning membrane protein which is the same as integrin-associated protein (IAP) and the ovarian tumour marker OA3. *Biochem. J.* 304:525–520.
35. McCormick, B. A., S. P. Colgan, C. Delp-Archer, S. I. Miller, and J. L. Madara. 1993. *Salmonella typhimurium* attachment to human intestinal epithelial monolayers: Transcellular signalling to subepithelial neutrophils. *J. Cell Biol.* 123:895–907.
36. McCormick, B. A., P. M. Hofman, J. Kim, D. K. Carnes, S. I. Miller, and J. L. Madara. 1996. Surface attachment of Salmonella Typhimurium to intestinal epithelia imprints the subepithelial matrix with gradients chemotactic for neutrophils. *J. Cell Biol.* In press.
37. Nash, S., J. Stafford, and J. L. Madara. 1987. Effects of polymorphonuclear leukocyte transmigration on barrier function of cultured intestinal epithelial monolayers. *J. Clin. Invest.* 80:1104–1113.
38. Nash, S., J. Stafford, and J. L. Madara. 1988. The selective and superoxide-independent disruption of intestinal epithelial tight junctions during leukocyte transmigration. *Lab. Invest.* 59:531–537.
39. Parham, P. 1983. Preparation and purification of active fragments from mouse monoclonal antibodies. *In* Immunological Methods in Biomedical Sciences. D. M. Weir, C. Blackwell, and L. Herzenberg, editors. Blackwell, Oxford. 14.1–14.2.
40. Parkos, C. A., C. G. Cochrane, M. Schmitt, and A. J. Jesaitis. 1985. Regulation of the oxidative response of human granulocytes to chemoattractants: no evidence for stimulated traffic of redox enzymes between endo and plasma membranes. *J. Biol. Chem.* 260:6541–6547.
41. Parkos, C. A., C. Delp, M. A. Arnaout, and J. L. Madara. 1991. Neutrophil migration across a cultured intestinal epithelium: dependence on a CD11b/CD18-mediated event and enhanced efficiency in the physiologic direction. *J. Clin. Invest.* 88:1605–1612.
42. Parkos, C. A., S. P. Colgan, and J. L. Madara. 1994. Interactions of neutrophils with epithelial cells: lessons learned from the intestine. *J. Amer. Soc. Nephrol.* 5:138–152.
43. Parkos, C. A., S. P. Colgan, A. E. Bacarra, A. Nusrat, C. Delp-Archer, S. Carlson, H. C. D. Su, and J. L. Madara. 1995. Intestinal epithelia (T84) possess basolateral ligands for CD11b/CD18 mediated neutrophil adherence. *Am J. Physiol.* 268:C472–C479.
44. Parsons, P. E., K. Sugahara, G. R. Cott, R. J. Mason, and P. M. Henson. 1987. The effect of neutrophil migration and prolonged neutrophil contact on epithelial permeability. *Am. J. Pathol.* 129:302–312.
45. Rosales, C., H. D. Gresham, and E. J. Brown. 1992. Expression of the 50-kDa integrin-associated protein on myeloid cells and erythrocytes. *J. Immunol.* 149:2759–2764.
46. Schwartz, M. A., E. J. Brown, and B. Fazeli. 1993. A 50-kDa integrin-associated protein is required for integrin-regulated calcium entry in endothelial cells. *J. Biol. Chem.* 268:19931–19934.
47. Senior, R. M., H. D. Gresham, G. L. Griffin, E. J. Brown, and A. E. Chung. 1992. Entactin stimulates neutrophil adhesion and chemotaxis through interactions between its Arg-Gly-Asp (RGD) domain and the leukocyte response integrin. *J. Clin. Invest.* 90:2251–2257.
48. Smith, C. W., S. D. Marlin, R. Rothlein, C. Toman, and D. C. Anderson. 1989. Cooperative interactions of LFA-1 and Mac-1 with intercellular adhesion molecule-1 in facilitating adherence and transendothelial migration of human neutrophils in vitro. *J. Clin. Invest.* 83:2008–2017.
49. Spertini, O., G. S. Kansas, J. M. Munro, J. D. Griffin, and T. F. Tedder. 1991. Regulation of leukocyte migration by activation of the leukocyte adhesion molecule-1 (LAM-1) selectin. *Nature (Lond.).* 349:691–694.
50. Springer, T. A. 1990. Adhesion receptors of the immune system. *Nature (Lond.).* 346:425–434.
51. Strohmeier, G. R., S. M. Reppert, W. I. Lencer, and J. L. Madara. 1995. The A2b adenosine receptor mediates cAMP responses to adenosine receptor agonists in human intestinal epithelia. *J. Biol. Chem.* 270:2387–2394.
52. Wright, S. D., P. E. Rao, W. C. van Voorhis, L. S. Craigmyle, K. Iida, M. A. Talle, E. F. Westberg, G. Goldstein, and S. C. Silverstein. 1983. Identification of the C3bi receptor of human monocytes and macrophages by using monoclonal antibodies. *Proc. Natl. Acad. Sci. USA.* 80:5699–5703.
53. Yardley, J. H. 1986. Pathology of idiopathic inflammatory bowel disease and relevance of specific cell findings: an overview. *In* Recent Developments in the Therapy of Inflammatory Bowel Disease. J. H. Yardley, editor. Johns Hopkins University Press, Baltimore, MD. 3–9.
54. Zhou, M., and E. J. Brown. 1993. Leukocyte response integrin and integrin-associated protein act as a signal transduction unit in generation of a phagocyte respiratory burst. *J. Exp. Med.* 178:1165–1174.